

RSC Advances



This is an *Accepted Manuscript*, which has been through the Royal Society of Chemistry peer review process and has been accepted for publication.

Accepted Manuscripts are published online shortly after acceptance, before technical editing, formatting and proof reading. Using this free service, authors can make their results available to the community, in citable form, before we publish the edited article. This *Accepted Manuscript* will be replaced by the edited, formatted and paginated article as soon as this is available.

You can find more information about *Accepted Manuscripts* in the [Information for Authors](#).

Please note that technical editing may introduce minor changes to the text and/or graphics, which may alter content. The journal's standard [Terms & Conditions](#) and the [Ethical guidelines](#) still apply. In no event shall the Royal Society of Chemistry be held responsible for any errors or omissions in this *Accepted Manuscript* or any consequences arising from the use of any information it contains.

Cite this: DOI: 10.1039/c0xx00000x

www.rsc.org/xxxxxx

ARTICLE TYPE

Highly selective and sensitive turn-on chemosensor for Al(III) ion at the nanomolar level in aqueous media and living organism

Siddhartha Pal,^a Buddhadeb Sen,^a Manjira Mukherjee,^a Mousumi Patra,^b Susmita Lahiri (Ganguly)^c and Pabitra Chattopadhyay^{a*}

5 Received (in XXX, XXX) Xth XXXXXXXXXX 20XX, Accepted Xth XXXXXXXXXX 20XX

DOI: 10.1039/b000000x

A highly sensitive and selective fluorescent reporter **L** for Al(III) ions was synthesized and characterized by physicochemical and spectroscopic tools along with single crystal X-ray crystallographic study. This is so far the first report of a crystallographically established fluorescence probe having two rhodamine units which make this probe as a highly sensitive towards Al(III) ions. **L** having high binding affinity towards Al(III) ions of $3.33 \times 10^8 \text{ M}^{-2}$ selectively detects Al(III) ions with almost no interference among various competitive, biologically relevant ions by a strong fluorescent (250 times) as well as colour change in HEPES buffer (1 mM, pH 7.4; acetonitrile/water: 1/3, v/v). The quantum yields (Φ) and molar extinction coefficient (ϵ) of $[\text{Al}_2(\text{L})_2(\text{CH}_3\text{CN})(\text{H}_2\text{O})(\text{NO}_3)_4](\text{NO}_3)_2$ (complex-1) were significantly greater than the sensor **L** for which this probe (**L**) can detect Al(III) ions as low as 3.26 nM comparable with the lowest LOD available in the literature. This non-cytotoxic probe (**L**) is also an efficient candidate to detect the intercellular distribution of aluminium ions in human lung cancer cells (A549) and Al(III) ions in matured tea leaves.

Introduction

20 The development of fluorescent chemosensors for selective detection and imaging of trace level metal ions is an attractive research area because of their simplicity, high sensitivity and real-time monitoring with a short response time.¹ For this purpose, the assessment of biologically active ions through fluorescence *turn-on* sensors still remains a challenging task. Aluminium being the third most abundant metallic element in the earth, has been proved to be a neurotoxic for a long time, and the abnormal accumulation of aluminium to all body tissues in humans and animals can cause many health hazards such as Parkinson's disease and Alzheimer's disease, colic and gastrointestinal problems, osteomalacia, rickets, interference with the metabolism of calcium, anaemia, and the risk of breast and lung cancer, even, it can damage the brains, liver and kidneys.² Several relevant aluminium compounds are extensively used in the paper, dye, textiles and food industry and as a component of many cosmetic preparations.³ Additionally, almost 40 % of soil acidity occurs from aluminium toxicity; moreover, high concentration of aluminium in ecosystem is toxic to plant, fish, algae and other species, and can enter into human body along with bio-cycle to cause other relevant diseases.⁴ The WHO (*World Health Organization*) prescribed the average human intake of aluminium as around 3-10 mg·day⁻¹ with a weekly dietary intake of 7 mg·kg⁻¹ body weight.^{4b,c}

45 Due to the potential impact of Al(III) ions on human health and the environment, detection and estimation of trace level aluminium ion is mandatory. Available standard techniques for

Al(III) ions detection with moderate sensitivity, such as chromatographic and spectrophotometric techniques, or atomic absorption or inductively coupled plasma atomic emission spectrometry are expensive and time-consuming in practice.³ Owing to weak coordination and strong hydration of Al(III) ions in water, coexistence of interfering ions is a problem.⁵ Therefore, highly selective and sensitive “turn-on” type fluorescence chemosensors for Al(III) ions are highly necessitated.

To the best of our knowledge, various fluorescent chemosensors have been reported for detection of Al(III) ions with moderate sensitivity to date⁶ including a very few reports of Al(III) ions sensors having two fluorophore units.^{6g,h} However, majority of the probes have limited solubility, tiresome synthetic efforts⁷ and lack of practical applicability in aqueous solutions.⁸ Thus, it is still highly demanding to develop new and superior methods for the selective estimation of Al(III) ions with high sensitivity and efficiency. Herein, we will report a highly sensitive non-cytotoxic cell permeable Al(III) ions selective chemosensor (**L**) having two identical fluorophore units for the enhancement of fluorescence through selective chelation of Al(III) ions in aqueous system. This probe (**L**) is quite useful to detect Al(III) ions in presence of huge amounts of several competitive ions and to congregate the mapping of the distribution of Al(III) ions in living cells.

Experimental

Materials and physical measurements

The analytical grade solvents and the other reagent grade chemicals used in this work were purchased from commercial sources and used as received. Here, throughout the experiments Milli-Q 18 Ω water was employed. A Shimadzu (model UV-1800) spectrophotometer was used for recording UV-vis spectra. IR spectra were recorded using Prestige-21 SHIMADZU FTIR spectrometer. A Perkin Elmer 2400 CHN elemental analyzer was utilized for elemental analyses (C, H and N). ^1H NMR spectra were collected from a JEOL 400 spectrometer using DMSO- d_6 solution and ^{13}C NMR spectra were collected from a Bruker Avance DPX 500 MHz spectrometer using CDCl_3 solution. All pH solutions were done by a Systronics digital pH meter (model 335) using either 50 mM HCl or NaOH solution. Electrospray ionization (ESI) mass spectra were recorded on a Qtof Micro YA263 mass spectrometer. Steady-state fluorescence emission and excitation spectra were recorded with a Hitachi-7000 spectrofluorimeter. Time-resolved fluorescence lifetime measurements were performed using a HORIBA JOBIN Yvon picosecond pulsed diode laser-based time-correlated single-photon counting (TCSPC) spectrometer from IBH (UK) at $\lambda_{\text{ex}} = 340$ nm and MCP-PMT as a detector. Emission from the sample was collected at a right angle to the direction of the excitation beam maintaining magic angle polarization (54.71). Maintaining the resolution of 28.6 ps per channel, the full width at half-maximum (FWHM) of the instrument response function was 250 ps. IBH DAS 6.2 data analysis software was used to fit the data to multiexponential functions after deconvolution of the instrument response function by an iterative reconvolution technique and here, reduced w_2 and weighted residuals served as parameters for goodness of fit.

The fluorescence property of **L** was checked in HEPES buffer (1 mM, pH 7.4; acetonitrile/water: 1/3, v/v) at 25 $^\circ\text{C}$. The pH study was carried out in 100 mM HEPES buffer solution by adjusting the pH using HCl or NaOH. *In vivo* study was performed at biological pH ~ 7.4 with 100 mM HEPES buffer solution. The stock solutions ($\sim 10^{-2}$ M) for the selectivity study of **L** towards different metal ions were prepared taking nitrate salts of sodium, potassium, copper(II), chromium(III), silver(I); acetate salt of manganese(II), zinc(II); chloride salts of nickel(II), cobalt(II), mercury(II), calcium(II), magnesium(II), iron(III); iron(II) sulphate in HEPES buffer (1 mM, pH 7.4; acetonitrile/water: 1/3, v/v) solvent. In this selectivity study the amount of these metal ions was a fifty times greater than that of the probe (**L**) used. Fluorimetric titration was performed with aluminium nitrate in HEPES buffer (1 mM, pH 7.4; acetonitrile/water: 1/3, v/v) solvent varying the metal concentration 0 to 150 μM and the probe concentration was 50 μM .

50 Preparation of **L**

Isophthalaldehyde (402.39 mg, 3.0 mmol) dissolved in methanol was added to the methanolic solution of *rhodamine-B hydrazide*^{13,14b} (2.79 mg, 6.1 mmol) at stirring condition. The resulting mixture was refluxed for 8 h. It was then evaporated to a small volume and cooled, from which white colored precipitate was filtered. The pure recrystallized product including the single crystals suitable for X-ray crystallographic

study were isolated from acetonitrile/methanol (3:1) mixed solvents on slow evaporation.

60 $\text{C}_{64}\text{H}_{66}\text{N}_8\text{O}_4$: M.P.: 250 ± 2 $^\circ\text{C}$. Anal. Found: C, 75.92; H, 6.39; N, 11.21; Calc.: C, 76.01; H, 6.58; N, 11.08. ESI-MS in methanol: $[\text{M} + \text{H}]^+$, m/z , 1011.9662 (100 %) (calcd.: m/z , 1011.5215), where M = molecular weight of **L** (Fig. S1 ESI †). IR (KBr, cm^{-1}): $\nu_{\text{C}=\text{C}}$ (aromatic), 2970; $\nu_{\text{C}=\text{O}}$, 1686; $\nu_{\text{CH}=\text{N}}$, 1613 (Fig. S2 ESI †). ^1H NMR (400 MHz, DMSO- d_6): 8.59 (s, 2H, CH=N); 7.90 (s, 1H); 7.86 (d, 1H, $J = 6.84$); 7.61-7.49 (m, 6H); 7.41 (s, 1H); 7.29-7.27 (m, 1H); 7.05 (d, 2H, $J = 7.64$); 6.39 (s, 4H); 6.34 (d, 4H, $J = 9.16$); 6.26 (d, 4H, $J = 8.4$); 3.46-3.12 (m, 16H, 8CH $_2$); 1.02-0.84 (m, 24H, 8CH $_3$) (Fig. S3 ESI †). ^{13}C NMR (δ , 76.99 MHz, ppm in CDCl_3): 165.13, 152.89, 152.22, 148.97, 146.23, 135.38, 135.37, 128.61, 128.22, 128.13, 127.99, 127.89, 127.63, 123.67, 123.39, 107.99, 105.75, 98.14, 65.85 (spirolactam carbon), 44.29, 29.67, 12.62 (Fig. S4B ESI †). Yield: 78%.

75 Synthesis of aluminium(III) complex, $[\text{Al}_2(\text{L})_2(\text{CH}_3\text{CN})(\text{H}_2\text{O})(\text{NO}_3)_4](\text{NO}_3)_2$ (complex-1)

To a solution of **L** in acetonitrile (1.0110 g, 1.0 mmol), aluminium(III) nitrate nonahydrate (in acetonitrile, 1125 mg, 3.0 mmol) was gently added dropwise and then the reaction mixture was stirred for 3.0 h at room temperature. A dark red precipitate was obtained after evaporation of the solvent by a rotary evaporator. It was then filtered, thoroughly washed with acetonitrile, and then dried in vacuum.

$[\text{C}_{66}\text{H}_{71}\text{Al}_2\text{N}_{13}\text{O}_{17}](\text{NO}_3)_2$: Anal. Found: C, 52.48; H, 4.44; N, 14.26; Calc.: C, 52.98; H, 4.78; N, 14.04. ESI-MS in acetonitrile: $[\text{M}]^+ = [\text{Z}^{2+}]/2$, m/z , 685.7311 (obsd. with 25 % abundance) (calcd.: m/z , 685.7361) where $[\text{Z}]^{2+} = [\text{Al}_2(\text{L})_2(\text{CH}_3\text{CN})(\text{H}_2\text{O})(\text{NO}_3)_4]^{2+}$ (Fig. S5). ^1H NMR (400 MHz, DMSO- d_6): 9.35 (2H broad); 8.41-8.32 (s, 2H, CH=N); 7.86 (broad, 2H); 7.58-7.52 (m, broad, 6H); 7.34 (s, 1H); 7.27-7.22 (m, 1H); 7.01 (broad, 2H); 6.37 (s, 4H); 6.30 (broad, 4H); 6.27 (broad, 4H); 3.69-3.22 (m, 16H, 8CH $_2$); 2.82 (s, CH $_3$ of acetonitrile); 0.97 (t, 24H, $J = 8.4$, 8CH $_3$) (Fig. S6 ESI †). ^{13}C NMR (δ , 76.99 MHz, ppm in CDCl_3): 165.33, 152.92, 152.62, 149.37, 146.53, 136.42, 135.37, 133.40, 128.24, 127.66, 123.69, 123.40, 108.12, 105.87, 98.24, 44.36, 29.66, 12.56 (Fig. S4A ESI †). Yield: 57%.

X-ray data collection and structural determination

X-ray data were collected on a Bruker's Apex-II CCD diffractometer using Mo $\text{K}\alpha$ ($\lambda = 0.71069$). The data were corrected for Lorentz and polarization effects and empirical absorption corrections were applied using SADABS from Bruker. A total of 14411 reflections were measured out of which 7333 were unique [$I > 2\sigma(I)$]. The structure was solved by direct methods using SIR-92⁹ and refined by full-matrix least squares refinement methods based on F^2 , using SHELX-97.¹⁰ All non-hydrogen atoms were refined anisotropically. All calculations were performed using Wingx package.¹¹ Important crystal and refinement parameters are given in Table S1.

110 Preparation of cell and in vitro cellular imaging with HL

Cell culture

A549, human lung cancer cell lines were obtained from National Center for Cell Science, Pune, India, and used throughout the experiments. Cells were grown in DMEM (Himedia) supplemented with 10% FBS (Himedia), and an antibiotic mixture (1.0 %) containing PSN (Himedia) at 37°C in a humidified incubator with 5.0 % CO₂ and cells were grown to 80-90% confluence, harvested with 0.025% trypsin (Himedia) and in phosphate-buffered saline (PBS), plated at the desired cell concentration and allowed to grow overnight before any treatment.

Cell imaging study

A549 cells were rinsed with PBS and incubated with DMEM containing Al-Sensor making the final concentration up to 10 μM in DMEM [the stock solution (3 mM) was prepared by dissolving Al-Sensor into DMSO] for 30 min at 37 °C. After incubation, bright field and fluorescence images of A549 cells were taken by a fluorescence microscope (Model: LEICA DM4000B, Germany) with an objective lens of 20X magnification. Similarly, fluorescence images of A549 cells (pre-incubated with 10 μM Al-Sensor) were taken with addition of different concentrations (10 μM-40 μM) of Al(NO₃)₂ salt at 10 minutes interval. A merged image between phase contrast and fluorescent image at 40 μM salt concentration were taken.

Cell cytotoxicity assay

In order to determine the cytotoxicity of Al-Sensor, 3-(4, 5-dimethylthiazol-2-yl)-2,5-diphenyltetrazolium bromide (MTT) assay was performed in A549 cells according to standard procedure^{12b}. Briefly, after treatment of overnight culture of A549 cells (10³ cells in each well of 96-well plate) with Al-Sensor (1.0, 10.0, 20.0 and 50.0 μM) for 6.0 h, 10.0 μl of a MTT solution (1mg/ml in PBS) was added in each well and incubated at 37°C continuously for 3.0 h. All media were removed from wells and 100 μl of acidic isopropyl alcohol was added into each well. The intracellular formazan crystals (blue-violet) formed were solubilized with 0.04N acidic isopropyl alcohol and absorbance of the solution was measured at 595 nm wavelength with a microplate reader (Model: THERMO MULTI SCAN EX). The cell viability was expressed as the optical density ratio of the treatment to control. Values are mean ± standard deviation of three independent experiments. The cell cytotoxicity was calculated as % cell cytotoxicity = 100% - % cell viability¹².

45 Results and discussion

Synthesis and characterization

The organic moiety (**L**) was synthesized by condensing a methanolic solution of *Isophthalaldehyde* and *rhodamine-B hydrazide* in 1:2 ratio (**Scheme1**). The data obtained from the physico-chemical and spectroscopic tools (ESI⁺), and the detailed structural analysis using single crystal X-ray crystallography are in accordance with the formulation of **L** as shown in **Scheme 1**. **L** is soluble in common polar organic solvents and sparingly soluble in water. The ESI mass

spectrum of the compound in methanol shows a peak at *m/z* 1011.9662 with 100% abundance assignable to [M + H]⁺ (calculated value at *m/z*, 1011.5215) where M = molecular weight of **L** (**Fig. S1** ESI⁺). The peaks obtained in ¹HNMR spectra of **L** have been assigned and these are good agreement with structural formula of the **L** in the solution state (**Fig. S3** ESI⁺). An ORTEP view and the packing arrangement of the probe **L** with the atom numbering scheme is illustrated in **Fig. 1** and **Fig. S7** (ESI⁺). The crystallographic data and the bond parameters (selected bond distances and angles) are listed in **Tables S1** and **S2**, respectively.

To establish the formation of complex-1 in solid state, it was isolated from the reaction of aluminium(III) nitrate with **L** respectively in 2:1 mole ratio in the acetonitrile medium. The complexes are soluble in methanol, DMSO, chloroform and acetonitrile etc. The peaks obtained in ¹H NMR of Al(III) complex have been assigned and it is in accordance with structural formula of the complex-1 as [Al₂(L)₂(CH₃CN)(H₂O)(NO₃)₄](NO₃)₂ (**Figs. S6** and **S8** ESI⁺).

Spectral characteristics

75 Absorption study

The electronic spectrum of **L** (50 μM) recorded in HEPES buffer (1 mM, pH 7.4; acetonitrile/water: 1/3, v/v) exhibited absorption bands at higher energy below 400 nm corresponding to π→π* (274 nm, ε = 1.34×10⁴) and n→π* (311 nm, ε = 9.8×10³) transitions. Incremental addition of aluminium(III) ions (0-150 μM) to the solution of **L** a new absorption peak at ca. 559 nm gradually developed due to the formation of a aluminium(III) complex with **L**. A visual colour change from colourless to red was appeared due to spiro lactam ring opening of **L** in complex-1 (**Fig. 2**). The molar extinction coefficient (ε) at 569 nm was increased from 8.5 (**L**) to 10⁴ (complex-1) which clearly indicated that the probe **L** is efficient colorimetric sensor for Al(III).

Emission study

The fluorescence spectra of **L** displayed no characteristic band emission at around 586 nm (λ_{ex} = 555 nm) (**Fig. 3**) in HEPES buffer (1 mM, pH 7.4; acetonitrile/water: 1/3, v/v). On stepwise addition of Al(III) ions (0-150 μM) to the solution of **L** (50.0 μM) caused a gradual increase (250 times) in the fluorescence intensity at ca. 586 nm with a slight red shift (**Fig. 3**) which was a considerable support of **L**-Al complex formation. Fluorescence quantum yields (Φ) were estimated (at λ_{ex} = 555 nm) by integrating the area under the fluorescence curves with the reported method.^{13,14} From where it is reflected that the quantum yields (Φ) of complex-1 was nearly 9 times greater than that of probe **L**, which clearly demonstrates the chelation-enhanced fluorescence (CHEF) process through spiro lactam ring opening.^{13,14b}

Job's plot analysis (**Fig. 3** inset,) showed that the complex-1 formed in solution state in a 1:2 [L:Al(III)] stoichiometric ratio. To evaluate the affinity of the probe towards Al(III) ions, the binding constant (K, 3.33 × 10⁸ M⁻²) was determined from the plot of (F_{max} - F₀)/(F_x - F₀) vs 1/[M]² (**Fig. S9**) using the modified Benesi-Hildebrand equation corresponding to 1:2 [L:Al(III)] stoichiometry.^{15,16}

$$(F_{\max} - F_0)/(F_x - F_0) = 1 + (1/K)(1/[M]^n)$$

where F_0 , F_x and F_{∞} are the emission intensities of organic moiety considered in the absence of Al(III) ions, at an intermediate Al(III) ions concentration, and at a concentration of complete interaction, respectively, and where $[C]$ is the concentration of Al(III) ions (here $n = 2$).

In addition to this dependency of occurring of CHEF, the selectivity of **L** towards Al(III) ions has also been verified by recording the fluorescence due to Al(III) ions even in the presence of 50 equivalent concentration of alkali and alkaline earth metal ions [Na(I), K(I), Mg(II), Ca(II)], and 50 equivalent concentration of several transition and other metal ions [Hg(II), Cr(III), Mn(II), Fe(III), Co(II), Ni(II), Cu(II), Zn(II), Cd(II) and Pb(II)] (Figs. S10 and S11 ESI†). This study reasonably reveals that **L** has almost no interference towards the detection of Al(III) ions with an excellent specificity to Al(III) ions over other cations.

To be acquainted with the role of pH on the fluorescence of **L**, the fluorescence intensities were measured at various pH values by adjusting the pH using HEPES buffer in presence and absence of Al(III) ions. In absence of Al(III) ions, the weak fluorescence intensity of **L** is almost independent over the pH range 6.0 to 10.0 (Fig. S12 ESI†); but at lower pH range (4.0 to 6.0), fluorescence intensity dramatically enhanced due to spiroactam ring opening. Again in presence of Al(III) ions the enhanced fluorescence intensity is also independent on the variation of pH over the range of pH 6.0 to 9.5. Here it is also noteworthy that **L**-Al species have much higher fluorescence intensity than only ring opened probe **L**, which clearly indicates the chelation-enhanced fluorescence (CHEF) process.

The fluorescence average lifetime measurement (at $\lambda_{em} = 586$ nm) of organic moiety (**L**) in presence and absence of Al(III) ions in HEPES buffer (1 mM, pH 7.4; acetonitrile/water: 1/3, v/v) medium showed the considerable increase in life time with increase of Al(III) ions concentration (Fig. 4). The average lifetimes were calculated to be 0.625 ns for only **L**, 1.189 ns for the mixture of **L**:Al(III) (1:2). Again the radiative rate constant k_r and total non-radiative rate constant k_{nr} of the organic moiety, **L** and Al(III) complex calculated from the equations: $\tau^{-1} = k_r + k_{nr}$ and $k_r = \Phi_f/\tau_s$ ¹⁷, were tabulated in Table S3. The data supported the fluorescent enhancement due to the increase of the ratio of k_r/k_{nr} from 0.091 for **L** to 3.16 for **L**-Al complex which indicate the more radiative decay pathway for **L**-Al complex.

NMR spectral study

To assure the above fact of the formation of the complex-1 and bonding pathway, we analysed the peaks in the observed ¹HNMR and ¹³CNMR spectral data of **L** and complex-1. The characteristic peaks in the ¹HNMR spectrum of **L** are almost identical with those in the spectra of complex-1 with a little change in some typical signals (Fig. S8 ESI†). On complexation with Al(III), the peaks due to the proton of -CH=N ($\delta = 8.59$ ppm) and the proton marked as 'a' viz. Fig. S8 ($\delta = 7.42$ ppm) obtained in the ¹HNMR spectrum of **L** shifted to the upfield by 0.18 ppm and 0.15 ppm respectively. All other peaks due to the hydrogens in ¹HNMR spectrum of **L** are

present in that of complex-1 with some slight changes for some protons. The peak at ca. 65.85 ppm attributable to spiroactam carbon (sp^3) observed in ¹³CNMR spectrum of **L** remarkably shifted to $\delta = 136.42$ ppm obtained in **L**-Al(III) complex due to the spiroactam rings opening. For this opening of the ring during complex formation, the sp^3 carbon converted to sp^2 hybridised carbon (Fig. S8 ESI). This study is in good agreement of the spiroactam ring opening mechanism during the coordination of **L** with Al(III) ions in the proposed fashion (Scheme 3).

Analytical figure of merit

The detection limit (LOD) was calculated from the calibration curve based on the fluorescence enhancement at 586 nm (Fig. 5) magnifying on the lower concentration region of Al(III) ions using the equation $3\sigma/S$, where the slope of the curve is S and σ_{zero} is the standard deviation of seven replicate measurements of the zero level^{14a,c} and it was found to be 3.26 nM. This observation clearly indicate the efficiency of this probe towards the detection of trace level Al(III) ions.

Aluminium detection in tea leaves

To explore the efficacy of this probe (**L**) for the detection of Al(III) ions in real sample, we examined the presence of aluminium in matured tea leaves. First the leaves were boiled in Milli-Q 18 Ω water and the leave extract was diluted by HEPES buffer (1 mM, pH 7.4). As the Al(III) ions present in tea leaves mainly in fluoride form¹⁸, so to solubilise it into aqueous citric acid was added in the extract keeping the pH fixed at 7.4 using buffer. Then 10^{-4} M probe (**L**) in acetonitrile was added into the extract. Visual and fluorescence color changes were observed and this surveillance clearly indicates the presence of Al(III) ions in tea leaves (Fig. S13).¹⁹

Cell Imaging

The cytotoxicity study (MTT assay) in human lung cancer cells treated with various concentrations of **L** for up to 6.0 h as shown in Fig. S14 showed that **L** concentrations up to 50.0 μ M did not show significant cytotoxic effects on human lung cancer cells for at least up to 6.0 h of its treatment. This study on A549 cells showed 91.52 % viability in presence of **L** compared to the control i.e. the sensor showed only 8.48 % cytotoxicity at 50.0 μ M concentrations. So this probe has been employed to detect the distribution of Al(III) ions in the living creature by acquiring the image by fluorescence microscope.

In fluorescence imaging studies, the **L** did not show any fluorescence itself in absence of Al(III) ions (Fig. 6B). However, addition of Al(III) ions to the cells (pre-incubated with 10 μ M of **L**) showed red fluorescence (Fig. 6C). Interestingly, the intensity of the fluorescence exhibited was a function of Al(III) ions ion concentration (Fig. 6C-6E). The intracellular Al(III) ions imaging behavior of **L** was studied on A549, human lung cancer cell lines by fluorescence microscopy. After incubation with **L** (10 μ M) at 37 °C for 30 min, the cells displayed no intracellular fluorescence (Fig. 6B). However, cells displayed light fluorescence with the addition of low concentration of aluminum ions (10 μ M) (Fig. 6C) and exhibited gradually intensive fluorescence when exogenous Al(III) ions was introduced into the cell via incubation with

solution of aluminium nitrate (Fig. 6D-6E). The fluorescence responses of **L** with various concentrations of added Al(III) ions proves that such fluorescence intensity can be used as indelible signature of selective sensor response clearly evident from the cellular imaging. Hence, these results indicate that **L** is an efficient candidate for monitoring changes in the intracellular Al(III) ions concentration under biological conditions.

Conclusion

In conclusion, a newly designed and structurally characterized rhodamine-isophthalaldehyde conjugate Schiff base (**L**) have been synthesized and characterised by physico-chemical and thorough spectroscopic analysis. **L** behaves as an aluminium ions selective chemosensor through CHEF process in HEPES buffer (1 mM, pH 7.4; acetonitrile/water: 1/3, v/v) over other competitive ions. The processes have nicely been established by the electronic, fluorimetric and NMR titration. This probe is also useful marker for Al(III) ions in human lung cancer cell lines (A549 cells) as **L** has no cytotoxicity. This is the first report so far of a crystallographically established probe having two rhodamine-fluorophore units to enhance the sensitivity parameter, consequently **L** showed a very low detection limit (LOD = 3.26 nM) towards Al(III) ions comparable with previous reports.^{5c,20} Compared to the reported probes,^{5c,20} this probe is however advantageous one in terms of the visible light excitation ($\lambda_{\text{ex}} = 555 \text{ nm}$) and red emission ($\lambda_{\text{em}} = 586 \text{ nm}$).

Acknowledgements

Council of Scientific and Industrial Research (CSIR) New Delhi, India is gratefully acknowledged for financial support. We deeply acknowledge Mr. Ajay Das and Prof. Samita Basu, Chemical Science Division, SINP, Kolkata, for allowing TCSPC instrument. S. Pal wishes to thank to state fund, West Bengal, India for offering the fellowships.

35 Notes and references

- ^aDepartment of Chemistry, Burdwan University, Golapbag, Burdwan-713104, West Bengal, India, E-mail: pabitracc@yahoo.com
^bDepartment of Biochemistry and Biophysics, University of Kalyani, Kalyani-741235, West Bengal, India.
^cInternational Centre for Ecological Engineering (ICEE), University of Kalyani, Kalyani, Nadia-741235, West Bengal, India
- †Electronic Supplementary Information (ESI) available: See DOI: 10.1039/b000000x/
[‡]CCDC 1403869 contains the supplementary crystallographic data for this paper. These data can be obtained free of charge from The Cambridge Crystallographic Data Centre via http://www.ccdc.cam.ac.uk/data_request/cif.
- 1 (a) G. de la Torre, G. Bottari, M. Sekita, A. Hausmann, D. M. Guldi and T. Torres, *Chem. Soc. Rev.*, 2013, **42**, 8049; (b) A. T. Wright and E. V. Anslyn, *Chem. Soc. Rev.*, 2006, **35**, 14.
 2 (a) D. P. Perl and A. R. Brody, *Science*, 1980, **208**, 297; (b) A. Becaria, A. Campbell and S. C. Bondy, *Toxicol. Ind. Health*, 2002, **18**, 309; (c) A. M. Pierides, Jr. W. G. Edwards, Jr. U. X. Cullum, J. T McCall and H. A. Ellis, *Kidney Int.*, 1980, **18**, 115.
 3 M. Mukherjee, S. Pal, S. Lohar, B. Sen, S. Sen, S. Banerjee, S. Banerjee and P. Chattopadhyay, *Analyst*, 2014, **139**, 4828.

- 4 (a) E. Alvarez, M. L. F. Marcos, C. Monterroso and M. J. F. Sanjurjo, *Ecol. Manag.*, 2005, **211**, 227; (b) J. Barcelo and C. Poschenrieder, *Environ. Exp. Bot.*, 2002, **48**, 75; (c) Z. Krejpcio and R. W. Wojciak, *Pol. J. Environ. Stud.*, 2002, **11**, 251; (d) T. P. Flaten and M. Odegard, *Food Chem. Toxicol.*, 1988, **26**, 959; (e) R. A. Yokel, *Neurotoxicology*, 2000, **21**, 813.
 5 (a) S. H. Kim, H. S. Choi, J. Kim, S. J. Lee, D. T. Quang and J. S. Kim, *Org. Lett.*, 2010, **12**, 560; (b) D. Maity and T. Govindaraju, *Chem. Commun.*, 2010, **46**, 4499; (c) K. K. Upadhyay and A. Kumar, *Org. Biomol. Chem.*, 2010, **8**, 4892; (d) Y. Zhao, Z. Lin, H. Liao, C. Duan and Q. Meng, *Inorg. Chem. Commun.*, 2006, **9**, 966.
 6 (a) Neeraj, A. Kumar, V. Kumar, R. Prajapati, S. K. Asthana, K. K. Upadhyay and J. Zhaob, *Dalton Trans.*, 2014, **43**, 5831; (b) S. Goswami, K. Aich, S. Das, A. K. Das, D. Sarkar, S. Panja, T. K. Mondal and S. Mukhopadhyay, *Chem. Commun.*, 2013, **49**, 10739 (c) Y. W. Liu, C. H. Chen and A. T. Wu, *Analyst*, 2012, **137**, 5201; (d) H. M. Park, B. N. Oh, J. H. Kim, W. Qiong, I. H. Hwang, K. D. Jung, C. Kim and J. Kim, *Tetrahedron Lett.*, 2011, **52**, 5581; (e) L. Wang, W. Qin, X. Tang, W. Dou, W. Liu, Q. Teng and X. Yao, *Org. Biomol. Chem.*, 2010, **8**, 3751; (f) J. Ren and H. Tian, *Sensors*, 2007, **7**, 3166; (g) S. B. Maity and P. K. Bharadwaj, *Inorg. Chem.*, 2013, **52**, 1161; (h) J. Hatai, M. Samanta, V. S. R. Krishna, S. Pal and S. Bandyopadhyay, *RSC Adv.*, 2013, **3**, 22572.
 7 (a) D. Maity and T. Govindaraju, *Chem. Commun.*, 2012, **48**, 1039; (b) D. Maity and T. Govindaraju, *Inorg. Chem.*, 2010, **49**, 7229; (c) Y. W. Wang, M. X. Yu, Y. H. Yu, Z. P. Bai, Z. Shen, F. Y. Li and X. Z. You, *Tetrahedron Lett.*, 2009, **50**, 6169 (d) W. Lin, L. Yuan and J. Feng, *Eur. J. Org. Chem.*, 2008, 3821.
 8 (a) Y. W. Choi, G. J. Park, Y. J. Na, H. Y. Jo, S. A. Lee, G. R. You and C. Kim, *Sensor Actuat B-Chem.*, 2014, **194**, 343; (b) K. B. Kim, D. M. You, J. H. Jeon, Y. H. Yeon, J. H. Kim and C. Kim, *Tetrahedron Lett.*, 2014, **55**, 1347.
 9 A. Altomare, G. Cascarano, C. Giacovazzo and A. Guagliardi, *J. Appl. Crystallogr.*, 1993, **26**, 343.
 10 G. M. Sheldrick, *Acta Cryst. A*, 2008, **A64**, 112.
 11 L. J. Farrugia, *J. Appl. Cryst.*, 1999, **32**, 837.
 12 (a) S. Banerjee, P. Prasad, A. Hussain, I. Khan, P. Kondaiah and A. R. Chakravarty, *Chem. Commun.*, 2012, **48**, 7702; (b) T. Mosmann, *J. Immunol. Methods*, 1983, **65**, 55.
 13 S. Pal, B. Sen, S. Lohar, M. Mukherjee, S. Banerjee and P. Chattopadhyay, *Dalton Trans.*, 2015, **44**, 1761 and references therein.
 14 (a) S. Lohar, S. Pal, B. Sen, M. Mukherjee, S. Banerjee, P. Chattopadhyay, *Anal. Chem.* **86**, 11357; (b) S. Pal, M. Mukherjee, B. Sen, S. Lohar and Pabitra Chattopadhyay, *RSC Adv.*, 2014, **4**, 21608 and refs. Therein; (c) S. Pal, M. Mukherjee, B. Sen, S. K. Mandal, S. Lohar, P. Chattopadhyay and K. Dhara, *Chem. Commun.*, 2015, **51**, 4410
 15 (a) H. A. Benesi and J. H. Hildebrand, *J. Am. Chem. Soc.*, 1949, **71**, 2703; (b) U. C. Saha, K. Dhara, B. Chattopadhyay, S. K. Mandal, S. Mondal, S. Sen, M. Mukherjee, S. V. Smaalen and P. Chattopadhyay, *Org. Lett.*, 2011, **13**, 4510.
 16 (a) K. Dhara, U. C. Saha, A. Dan, M. Manassero, S. Sarkar and P. Chattopadhyay, *Chem. Commun.*, 2010, **46**, 1754; (b) S. Pal, M. Mukherjee, B. Sen, S.K. Mandal, S. Lohar, P. Chattopadhyay and K. Dhara, *Chem. Commun.*, 2015, **51**, 4410; (c) U. C. Saha, B. Chattopadhyay, K. Dhara, S. K. Mandal, S. Sarkar, A. R. Khuda-Bukhsh, M. Mukherjee, M. Helliwell and P. Chattopadhyay, *Inorg. Chem.*, 2011, **50**, 1213; (d) B. Sen, M. Mukherjee, S. Pal, S. K. Mandal, M. S. Hundal, A. R. Khuda-Bukhsh, *RSC Advances*, **4**, 15356; (e) M. Mukherjee, B. Sen, S. Pal, M. S. Hundal, S. K. Mandal, A. R. Khuda-Bukhsh and P. Chattopadhyay, *RSC Advances*, 2013, **3**, 19978.
 17 (a) N. J. Turro, *Modern Molecular Photochemistry*; Benjamin/Cummings Publishing Co., Inc.: Menlo Park, CA, 1978, 246; (b) J. R. Lakowicz, *Principles of Fluorescence Spectroscopy*, Springer 2006.

- 18 H. J. Gao, Q. Zhao, X. C. Zhang, X. C. Wan, and J. D. Mao, *J. Agric. Food Chem.*, 2014, **62**, 2313.
- 19 (a) R. Tolra, K. V. Mikus, R. Hajiboland, P. Kump, P. Pongrac, B. Kaulich, A. Gianoncelli, V. Babin, J. Barcelo, M. Regvar and C. Poschenrieder, *J Plant Res.*, 2011 **124**, 165; (b) J. Ruan and M. H. Wong, *Environmental Geochemistry and Health*, 2001, **23** 53.
- 20 (a) K. Tiwari, M. Mishra and V. P. Singh, *RSC Adv.*, 2013, **3**, 12124; (b) M. Mukherjee, B. Sen, S. Pal, S. Banerjee, S. Lohar and P. Chattopadhyay, *RSC Adv.*, 2014, **4**, 64014.

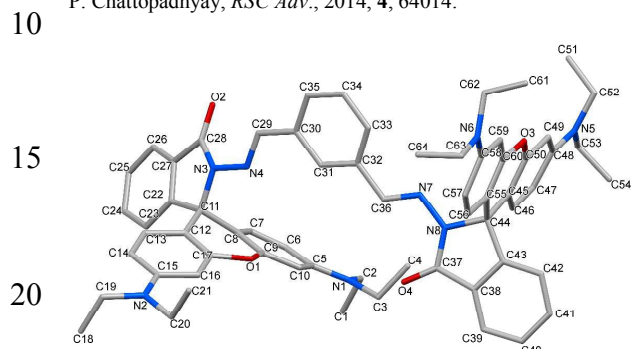


Fig. 1 Molecular views of **L** with atom numbering scheme. Hydrogen atoms are omitted for clarity.

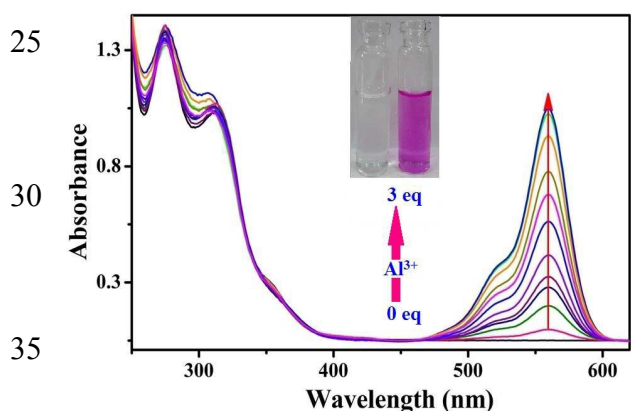


Fig. 2 UV-Vis titration spectra of **L** with Al(III) ions in HEPES buffer (1 mM, pH 7.4; acetonitrile/water: 1/3, v/v) at 25 °C. Inset shows the visual color change of **L** and **L** + Al(III) (1:2)

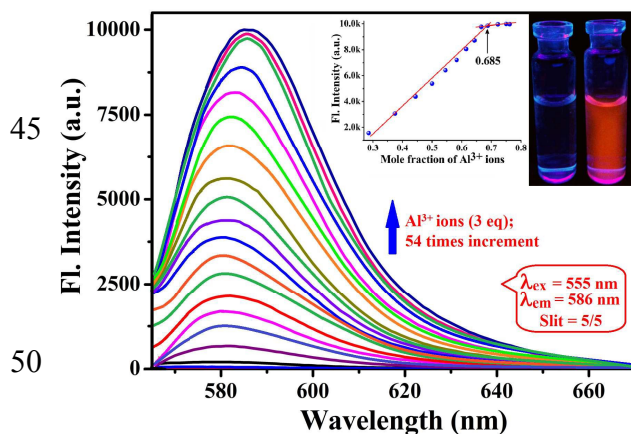


Fig. 3 Fluorescence titration of **L** with gradual addition of Al(III) ions in HEPES buffer (1 mM, pH 7.4; acetonitrile/water: 1/3, v/v) at 25 °C. Inset shows 1:2 (**L**:**Al**) stoichiometry by Job's plot and the fluorescence colour change of **L** and **L** + Al(III) (1:2)

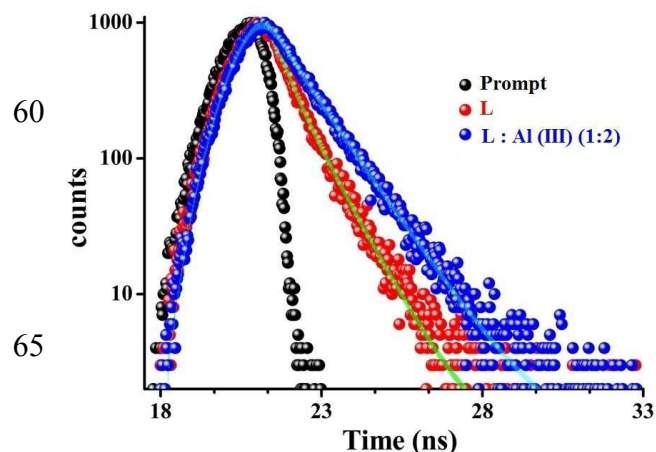


Fig. 4 Fluorescence life time decay profiles of **L** and **L** : Al(III) (1:2) at 586 nm with a Nano-LED of 550 nm as the light source

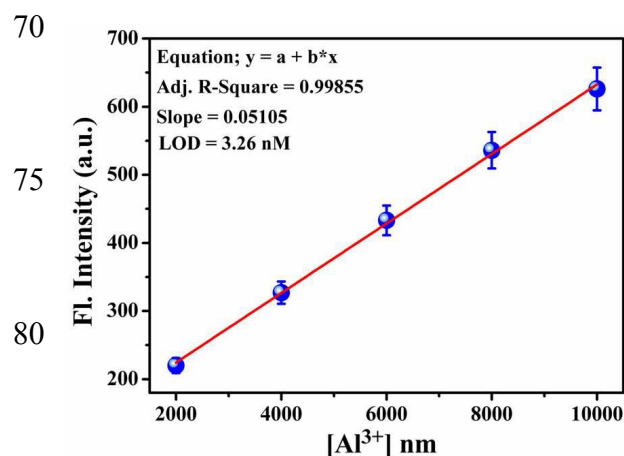


Fig. 5 Calibration curve for the nanomolar range, with error bars for calculating the LOD of Al(III) by **L** in HEPES buffer (1 mM, pH 7.4; acetonitrile/water: 1/3, v/v) at 25 °C

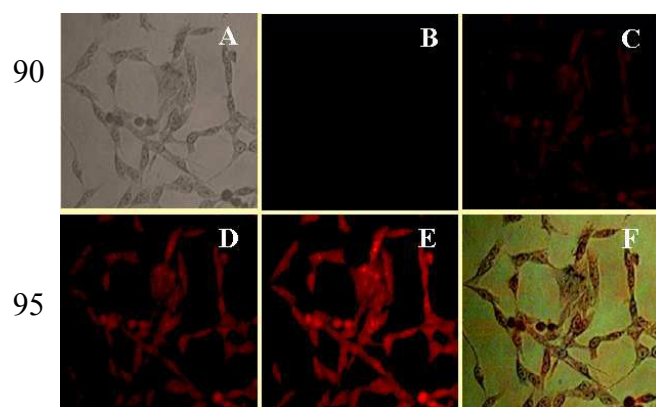
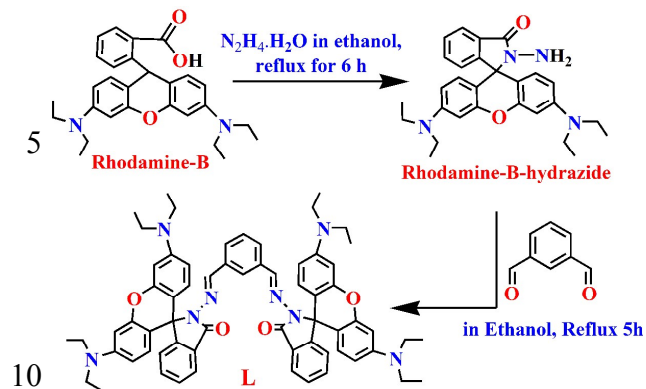
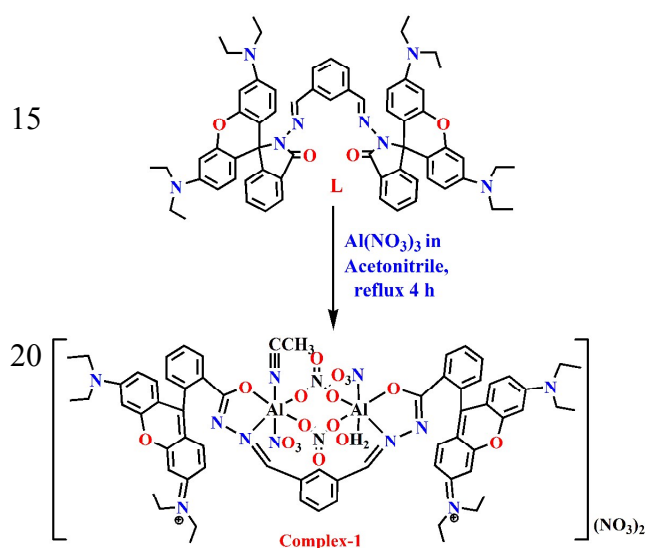


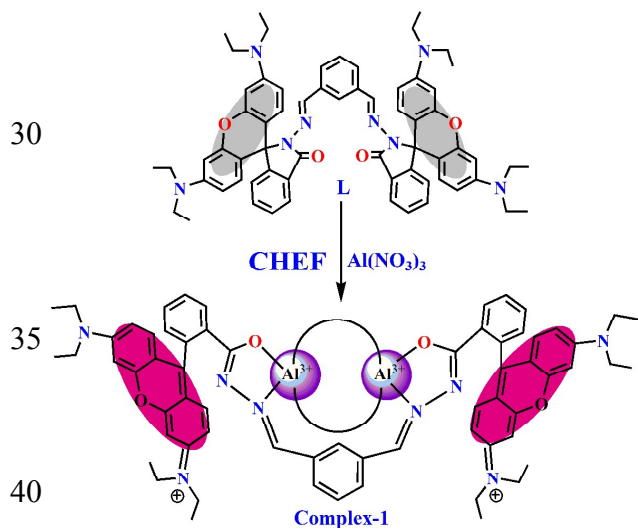
Fig. 6 (A) Phase contrast, (B) fluorescence image of A549 cells incubated with 10 μM **L** for 30 min at 37°C. **L** (10 μM) incubated cells were washed with PBS and were exposed to the presence of sequentially increased concentrations of added extracellular Al(III) ions as (C) 10 μM , (D) 20 μM and (E) 40 μM . (F) represent the merge image of phase contrast and fluorescence image. For all imaging, the samples were excited at 555 nm



Scheme 1 Schematic representation of synthesis of the probe L



25 Scheme 2 Schematic representation of synthesis of the complex-1



Scheme 3 Plausible mechanistic pathway of L for sensing of Al(III)

Graphical abstract

A newly synthesized and crystallographically characterized rhodamine-isophthalaldehyde conjugate Al(III) ions selective chemosensors (**L**) detects the Al(III) ions by colorimetrically as well as fluorimetrically with a high sensitivity (3.26 nM) in HEPES buffer (1 mM, pH 7.4; acetonitrile/water: 1/3, v/v). This non-cytotoxic probe is useful to detect the intercellular distribution of Al(III) ions in human lung cancer cells (A549) and also competent to detect Al(III) ions in tea extract.

